Adv. Polar Upper Atmos. Res., **13**, 89–104, 1999

DISTORTION OF THE OUTER BOUNDARY OF THE CLOSED REGION IN THE TSYGANENKO MAGNETIC FIELD MODEL

Takashi YAMAMOTO[1], Shoshi INOUE[2], Masao OZAKI[3] and Nozomu NISHITANI[4]

[1] *Department of Earth and Planetary Physics, University of Tokyo, Hongo 7-chome, Bunkyo-ku, Tokyo 113-0033*
[2] *Aichi College of Technology, Manori, Nishihazama-cho, Gamagori 443-0047*
[3] *Institute of Industrial Science, University of Tokyo, Roppongi 7-chome, Minato-ku, Tokyo 106-8558*
[4] *Solar-Terrestrial Environment Laboratory, Nagoya University, Honohara, Toyokawa 442-8507*

Abstract: Using the Tsyganenko magnetic field model (TSYGANENKO, Planet. Space Sci., **37**, 5, 1989) we make an attempt to determine the outer boundary of the closed region when the interplanetary magnetic field (IMF) is southward. As a simple magnetic field model including the effect of IMF $B_Z<0$, the B_Z component of a constant value of minus a few nanoTeslas is added to the magnetic field in the Tsyganenko model with low K_p values. In this paper, if the magnetic field strength, B, is not less than 2 nT in the whole range of a field line (namely the minimum B along a field line is greater than 2 nT), this field line is judged to be "firmly" closed. The firmly closed field lines are thought to be definitely closed as long as the fluctuation amplitude of B_Z (around its average level) in the interplanetary (solar wind) magnetic field is less than 2 nT. The outer boundary of the firmly closed region is then constituted by field lines with the minimum B of 2 nT. This boundary is found to be close to (just inside of) the open-closed boundary, which can be determined with accuracy of 0.01° in latitude of the foot point of a field line. It is found that a circle with the center at a latitude of about 85° on the midnight meridian can be fitted to the outer boundary of the firmly closed region, as it is projected to the ionosphere. Interestingly this circle coincides with a typical auroral circle; the auroral circles are those delineating the poleward boundary of the quiet auroral belt, which were earlier identified from the statistical analysis of satellites' auroral images by MENG *et al.* (J. Geophys. Res., **82**, 164, 1977). Importantly we find that the outer boundary of the firmly closed region is "distorted" on the nightside in the sense that the ionospheric projection of the average magnetic drift velocity of a plasma with isotropic pressure is not parallel to the boundary; more specifically, that of an isotropic ion fluid has an equatorward component on the duskside boundary and a poleward one on the dawnside boundary, respectively. This kind of the boundary distortion may be one of the possible causes of the generation of the nightside region 1 field-aligned current, which has been first suggested by HRUŠKA (J. Geophys. Res., **91**, 371, 1986) and recently, further studied by YAMAMOTO and INOUE (Proc. NIPR Symp. Upper Atmos. Phys., **11**, 106, 1998).

1. Introduction

The determination of the open-closed field line boundary is one of the fundamental issues in magnetospheric physics. Attempts to determine the open-closed boundary using the Tsyganenko magnetic field models (TSYGANENKO, 1987, 1989) have been made by several authors (*e.g.*, BIRN *et al.*, 1991; ELPHINSTONE *et al.*, 1991; NISHITANI, 1992). BIRN *et al.* simply assumed that the field lines extending down to $X = -70\,R_E$, which is the tailward validity limit of TSYGANENKO's (1987) long model, are open. (In this paper, we use the solar-magnetospheric coordinates (X, Y, Z).) When the IMF B_Z is near zero or northward (hereafter this condition is referred to as "nonsouthward IMF"), the distant neutral line or separatrix has been inferred to lie beyond $X = -70\,R_E$ (*e.g.*, TSURUTANI *et al.*, 1984; ZWICKL *et al.*, 1984). Even if the separatrix lies around $X = -200\,R_E$, its location projected to the ionosphere turns out to be close to the ionospheric projection of the line of $X = -70\,R_E$ on the equatorial plane, due to mapping along the field lines highly converging in the radial dimension. Thus the ionospheric projection of the equatorial line at $X = -70\,R_E$ may be regarded as a first approximation to the open-closed boundary on the ionospheric plane under the nonsouthward IMF condition. In fact, as was discussed by BIRN *et al.*, the poleward boundary of the auroral luminosity in such a condition sometimes takes a teardrop shape, which is similar to that of the open-closed boundary based on the TSYGANENKO (1987) long model.

ELPHINSTONE *et al.* (1991) similarly assumed that the open field lines are those extending beyond some specific bounds far away from the Earth. NISHITANI (1992) defined the open field lines to reach the cylindrical surface of square root of $\sqrt{X^2+Y^2} =$ (*e.g.*,) $35\,R_E$ or the planes at $Z = \pm$(*e.g.*,) $25\,R_E$, starting from the Earth surface. (In his analysis the dipole tilt effect was neglected.) A basic idea underlying all these models is described as follows: If the magnetic field strength along a field line drops down to about 1 nT, this field line tends to merge into one originating from the solar wind, *i.e.*, the interplanetary field line, because the magnetic field strength in the solar wind is normally of the order of 1 nT. Hence this field line may be regarded as open. In this paper, following this idea more faithfully than in the previous works (as will be explained later), we make an attempt to determine the outer boundary of the closed region.

In case of the southward IMF B_Z, if it penetrates, to some degree, inside the magnetosphere, the open-closed boundary is assumed to be located nearer to the Earth compared with that in case of nonsouthward IMF B_Z. (In this paper the effects of the IMF B_Y and B_X are not considered, and these components are implicitly assumed zero.) Namely, the open region (or polar cap) on the ionospheric plane is extended to lower latitudes as the IMF B_Z turns southward, as has been evidenced from the observed particle precipitation (*e.g.*, AKASOFU *et al.*, 1992). In the Tsyganenko model (except its recent versions (TSYGANENKO, 1995)), however, all the field lines within its validity limits are closed so that the open-closed boundary cannot be defined. Therefore, as a simplest model to include the IMF B_Z effect it may be appropriate to externally add a constant B_Z component (later, referred to as $B_{Z,\,\mathrm{ext}}$) to the original field from the Tsyganenko model. Upon such modification it is possible to explicitly determine the open-closed boundary which would lie within the validity limit of the Tsyganenko model. (In principle, it is impossible to determine the exact location of the open-closed boundary because any field line cannot be drawn from the separatrix where the magnetic field vanishes. Practically, however, with a given level of numerical accuracy we can determine the approximate location of the separator between the open and closed field lines.) Taking into account the IMF fluctuation around a certain average (say, over one hour) level, the more meaningful concept we propose here is the "firmly" closed region where any field line is invariably closed, being unperturbed by temporal IMF fluctuations with amplitudes of the order of 1 nT. Practically, we assume that the outer boundary of the firmly closed region is constituted by the field lines on which minimum values of the magnetic field strength are about 2 nT.

The purpose of the present paper is to show that in case of southward IMF B_Z, the outer boundary of the firmly closed region is distorted on the nightside. The distortion means that the ionospheric projection of the average magnetic drift velocity of an isotropic ion fluid has an equatorward component on the duskside boundary and a poleward one on the dawnside, respectively. The outer boundary of the firmly closed region is determined using the TSYGANENKO (1989) model with low K_p values, no dipole tilt, and southward IMF B_Z of minus a few nanoTeslas externally added. (In our study the dipole field is used as the contribution from Earth-internal sources.) This boundary is found to be just inside the open-closed boundary with difference less than about 1° in latitude of the field line foot point. Interestingly, the outer boundary of the firmly closed region is found to coincide with a typical auroral circle; the auroral circles have been identified as those delineating the poleward boundary of the auroral belt, from the Defense Meteorological Satellite Program (DMSP) satellites' auroral images (MENG *et al.,* 1977). More importantly, by calculating the flux tube volume on the outer boundary of the closed region we find that the ionospheric projection of the average magnetic drift velocity of an isotropic ion fluid has an equatorward component on the duskside of that boundary and a poleward one on its dawnside, respectively. This fact may be regarded as a signature of the convection-distortion of that boundary, which was earlier suggested as a possible generation mechanism for the nightside region 1 field-aligned current (FAC) (HRUŠKA, 1986; YAMAMOTO and INOUE, 1998). In Section 3, we make a rough estimation of the intensity of the region 1 FAC generated near the outer boundary of the closed region. In this respect, notably the EXOS-D MGF data first reveal that the region 1 FACs are often concentrated on a narrow ($<1°$ in latitude) zone near the high-latitude boundary of the auroral oval. This finding is presented in our subsequent paper (this issue).

2. Outer Boundary of the Closed Region

Figure 1 shows the equicontours of $B=B_Z=2$ nT in the equatorial (X-Y) plane, in three cases of $B_{Z,\,\mathrm{ext}}=0$, -2, and -4 nT, where the Z-component of the magnetic field, $B_{Z,\,\mathrm{ext}}$ (representing the IMF B_Z), is uniformly added to the original magnetic field from the 1989 version of Tsyganenko model with $K_p=0$ and no dipole tilt. (Note that the magnetic field at the equator has only a Z-component because the field lines in our model are symmetric with respect to the X-Y plane. They are also symmetric with respect to

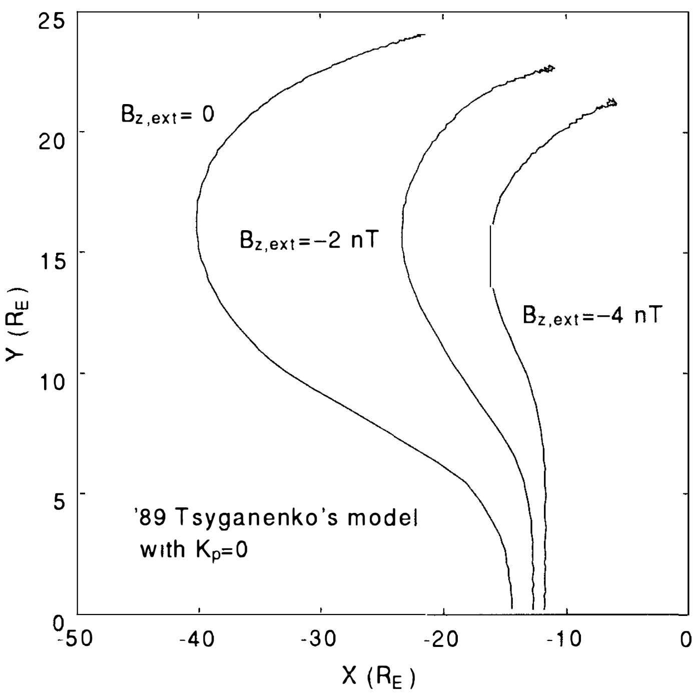

Fig. 1. *Equicontours of '$B=B_{eq}=2\,nT$' in the X-Y plane, for three cases of $B_{Z,ext}=0$, -2 and $-4\,nT$. The local time ranges of the contours are such that their (field-aligned) projections to the ionosphere (see Fig. 2) range between 24 and 15 MLT. Coordinates X and Y are in units of the Earth radius, R_E.*

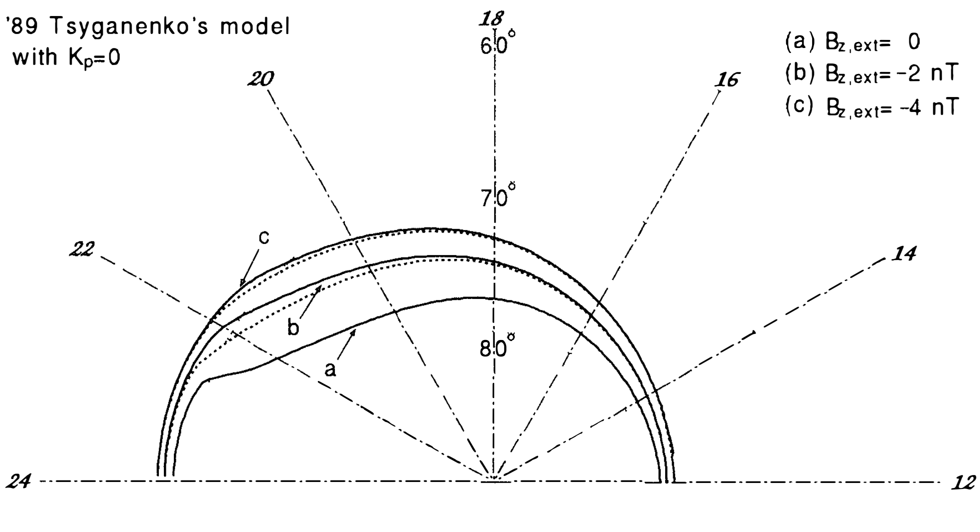

Fig. 2. *Solid lines show the ionospheric footprints of the $B_{eq}=2\,nT$ lines in Fig. 1, for (a) $B_{Z,ext}=0$, (b) $B_{Z,ext}=-2\,nT$ and (c) $B_{Z,ext}=-4\,nT$, and dotted lines show the open-closed boundaries in cases of (b) and (c). Dial of MLT (12–24) and lines of 60°, 70° and 80° magnetic latitudes are indicated.*

the *Z-X* plane. Hence, in this paper (except for Figs. 5 and 9), we show only the duskside half of the two-dimensional plots of various quantities in the equatorial and ionospheric planes.) Figure 2 (solid lines) shows the footprints of these equicontours of

'$B_{eq}=2$ nT' in the three cases; namely they are obtained by mapping the equicontours in Fig. 1, along the field lines, onto the ionospheric plane. Also indicated (by dotted lines) are the open-closed boundaries in cases of $B_{Z,\,ext}\neq 0$, which are determined with accuracy of 0.01° in latitude of the footprint. (As is mentioned in introduction, the open-closed boundary cannot be defined for $B_{Z,\,ext}=0$.) In Fig. 3 a few field lines near the open-closed boundary are drawn in the midnight meridional (Z-X) plane, for the case of $B_{Z,\,ext}=-4$ nT. In principle, by drawing field lines with the foot point latitudes at intervals of $\Delta\theta$, it is possible to determine the open-closed boundary with accuracy of $\Delta\theta$. In the present study, $\Delta\theta$ is taken to be 0.01°.

Since every closed field line has a minimum value of the magnetic field strength at the equator, according to our definition of the firmly closed region (see introduction), each contour of $B_{eq}=2$ nT in Fig. 2 is the footprint of the outer boundary of that region. As was discussed by TSYGANENKO (1995), the equatorial (middle to distant) tail B_Z values in the '89 Tsyganenko model are inaccurate. For this reason, the outer boundary of the firmly closed region in Fig. 2 is not meaningful for the case of $B_{Z,\,ext}=0$. In the following we focus our discussion on the case that $B_{Z,\,ext}$ is minus a few nanoTeslas.

From Fig. 2 it is found that the outer boundary of the firmly closed region is just equatorward of the open-closed boundary, and that the difference in latitude between these two boundaries is at most about 1° for $B_{Z,\,ext}=-2$ nT and about 0.4° for $B_{Z,\,ext}=-4$ nT. A circle with the center at a latitude of about 85° on the midnight meridian can be well fitted to the outer boundary of the firmly closed region for $B_{Z,ext}=-4$ nT. Such fitting is illustrated in Fig. 4. Interestingly, this circle coincides with a typical auroral circle; the auroral circles are those fitted to the poleward boundary of the auroral belt photographed from the DMSP satellites (MENG *et al.*, 1977), which are shown in Fig. 5. In this context, it is worthy of noting that the most poleward (nightside)

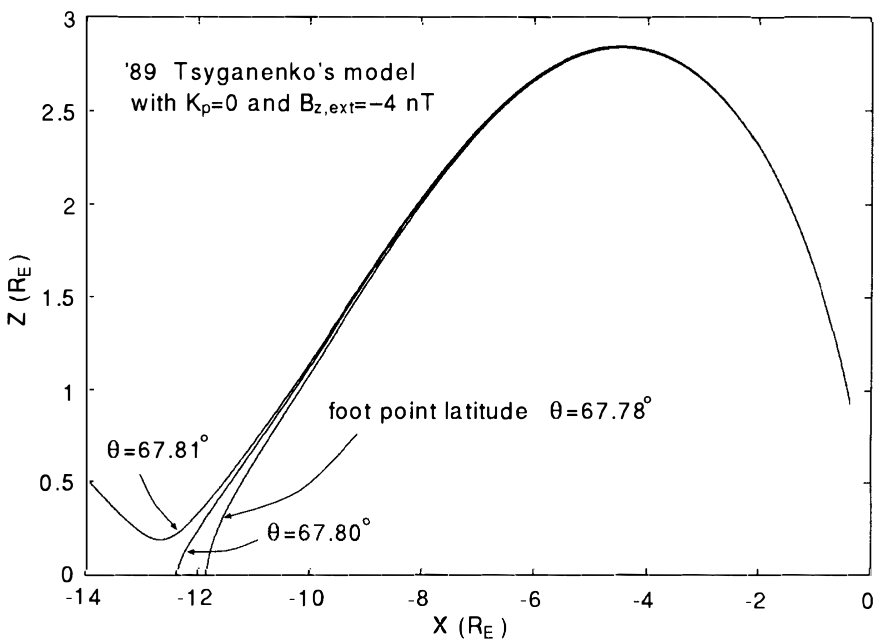

Fig. 3. Field lines near the separatrix in the Z-X plane, for the case of $B_{Z,\,ext}=-4$ nT.

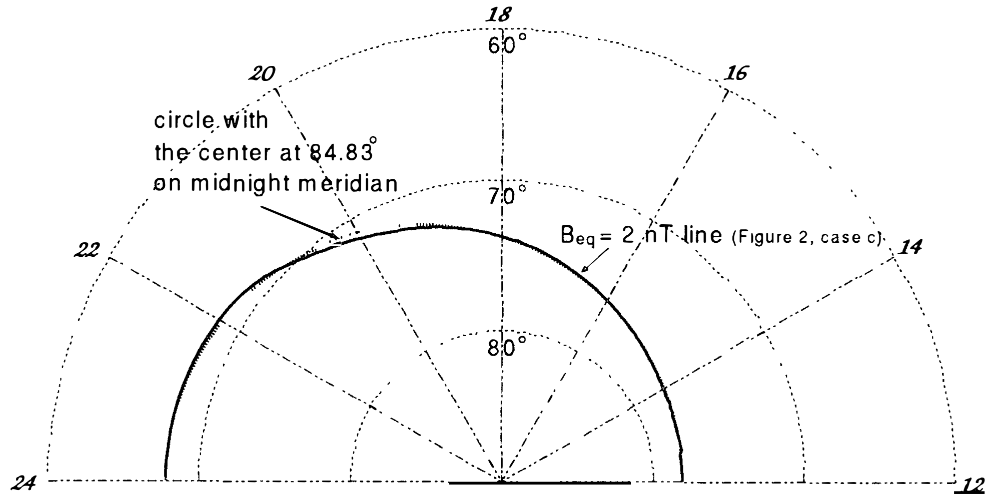

Fig. 4. Comparison of the $B_{eq}=2\,nT$ line with a typical auroral circle with the center at a latitude of about 85° on the midnight meridian.

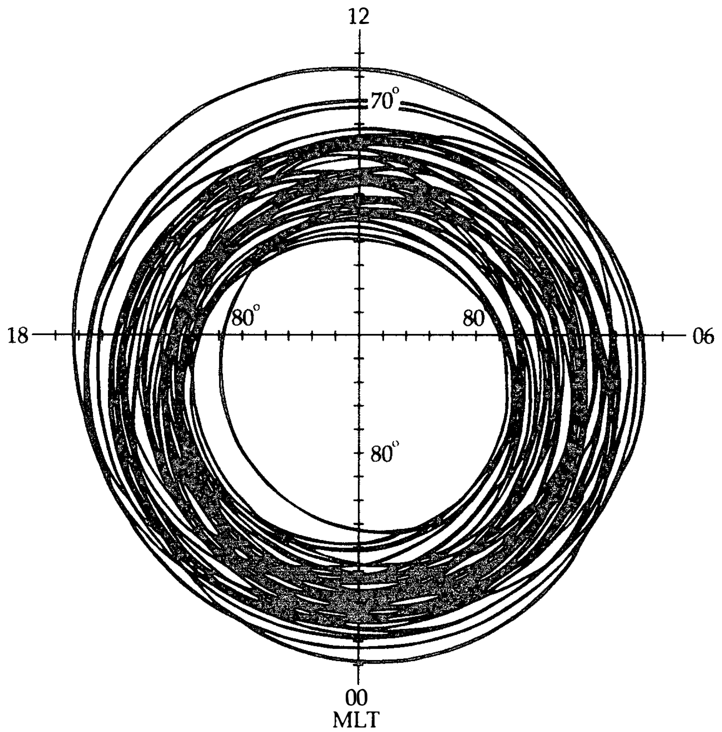

Fig. 5. Auroral circles fitted to the poleward boundary of the auroral belt photographed from the DMSP satellites, a reproduction of Fig. 6 in MENG et al. (1977). The centers of the auroral circles were found to be concentrated within a circular area of 3° radius centered at ~4.2° away from the geomagnetic pole along the 0010 MLT (nearly midnight) meridian (see Fig. 5a in their paper).

discrete aurora is observed just equatorward of the open-closed boundary with a gap of ~0.5° in latitude (YAMAMOTO *et al.*, 1993; FUKUNISHI *et al.*, 1993).

Finally we touch on the difference in the footprint between the $B_{eq}=2$ nT line and the $B_{eq}=1$ nT or 3 nT line. Figure 6 shows the $B_{eq}=1$ nT, 2 nT and 3 nT lines in cases

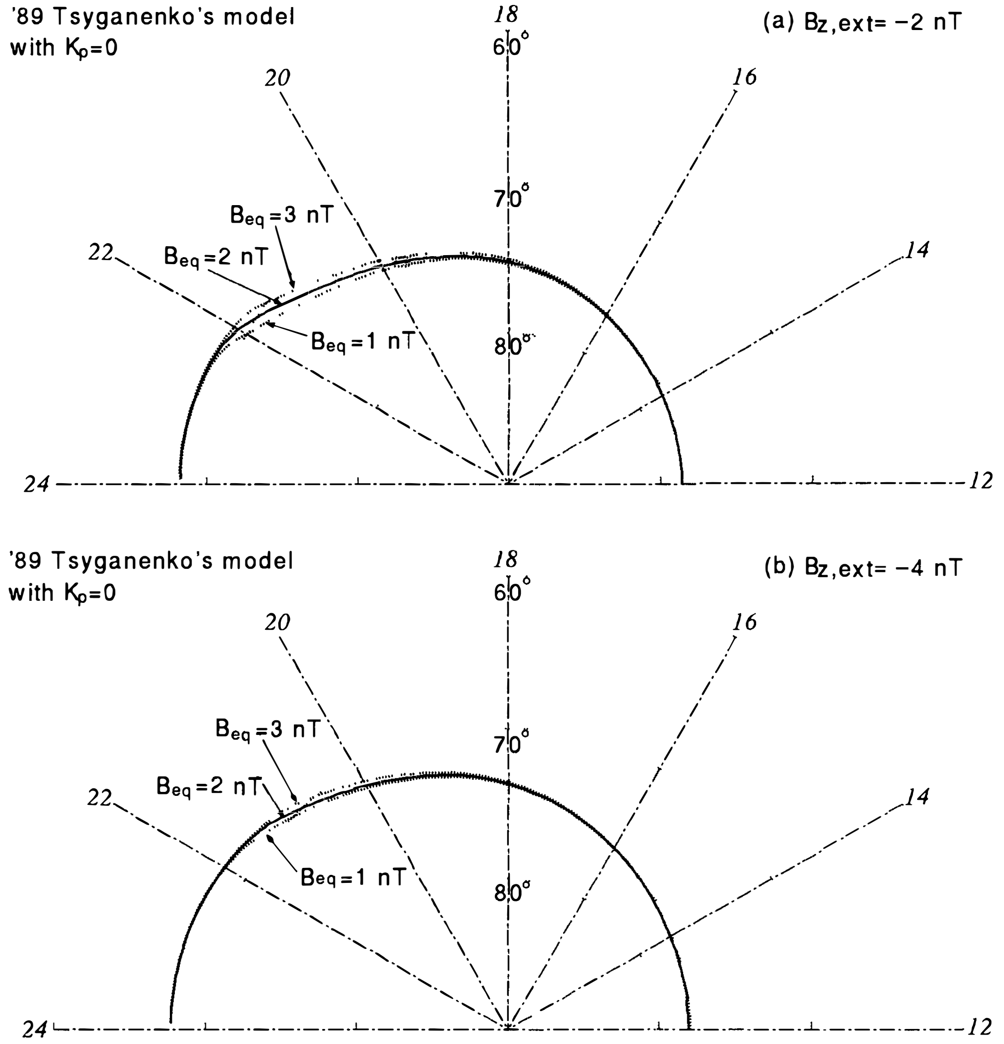

Fig. 6. Ionospheric footprints of the $B_{eq}=1$ nT, 2 nT and 3 nT lines for (a) $B_{Z,\,ext}=-2$ nT and (b) $B_{Z,\,ext}=-4$ nT, both for $K_p=0$.

of (a) $B_{Z,\,ext}=-2$ nT and (b) $B_{Z,\,ext}=-4$ nT, both for $K_p=0$. In case (a), the difference in latitude between the $B_{eq}=2$ nT line and the $B_{eq}=1$ nT or 3 nT line is at most about 0.6°, and in case (b) it is at most about 0.4°.

3. Magnetic Drift Velocity on the Outer Boundary of the Closed Region

In this section we examine the average magnetic drift velocity of charged particles on the outer boundary of the firmly closed region. This drift velocity can be crucial for charge separation around that boundary, because the energy density of particles is much changed across it, during the period of the IMF $B_Z<0$ (the condition studied in this paper). As is discussed by YAMAMOTO and INOUE (1998), under this IMF condition the energy density greater inside than outside of the closed region occurs due to the facts that particles can be nonadiabatically energized by the dawn to dusk electric field just after they are injected into the nightside closed region, and that they escape along the field lines to the interplanetary space after leaving the closed region. Actually the

EXOS-D satellite observations (*e.g.*, SAITO *et al.*, 1992) identified the accelerated ion beams at the poleward edge of the auroral precipitation region between 20 MLT and 4 MLT. From the AMPTE/IRM satellite data, BAUMJOHANN *et al.* (1990) showed the MLT-dependence of the occurrence rate of a high-speed (>400 km/s) ion beam: the occurrence rate is peaked around midnight and it decreases toward dusk or dawn. From this fact, we can expect that on average, the energy density of ions (including beams) is greater in the midnight sector than in the dawn/dusk sectors. In the present paper, as a first approximation, the outer boundary of the firmly closed region in the 20–4 MLT range (, which is represented by the $B_{eq}=2$ nT line in this MLT range) is identified with the nightside injection boundary. (The injection boundary here is defined such that the ions entering the closed region, through the boundary, can be immediately accelerated, nonadiabatically, from several hundred eV to keV energies.)

Assuming that the plasma pressure, p, is isotropic and uniform along the field lines, the (quasi-steady) FAC density $J_{\parallel \mathrm{I}}$ at the ionospheric height can be given by (YAMAMOTO *et al.*, 1996)

$$J_{\parallel \mathrm{I}}=e\bar{\nu}_{\mathrm{m,I}}\cdot \nabla_{\mathrm{I}}\varepsilon, \tag{1}$$

where e (>0) is the electronic charge, ∇_{I} denotes the gradient on the ionospheric plane, and the positive value of $J_{\parallel \mathrm{I}}$ is for the FAC flowing away from the ionosphere, *i.e.*, the upward FAC. Here ε is the flux tube energy content, which is defined as the total kinetic energy of the plasma particles contained in a flux tube with unit cross-sectional area at the ionospheric height:

$$\varepsilon=\int_{s_{\mathrm{I}}}^{s_{\mathrm{e}}}\frac{3p}{2}\frac{B_{\mathrm{I}}}{B(s)}\,\mathrm{d}s,$$

and $\bar{\nu}_{\mathrm{m,I}}$ is the averaged value of the ionospheric projection of the magnetic drift velocity per unit energy, which is defined as

$$\bar{\nu}_{\mathrm{m,I}}=\frac{1}{R_b}\int_{s_{\mathrm{I}}}^{s_{\mathrm{e}}}\frac{V_{\mathrm{m,I}}(s)}{W}\frac{B_{\mathrm{I}}}{B(s)}\,\mathrm{d}s \text{ and } R_b=\int_{s_{\mathrm{I}}}^{s_{\mathrm{e}}}\frac{B_{\mathrm{I}}}{B(s)}\,\mathrm{d}s, \tag{2}$$

where $V_{\mathrm{m,I}}(s)$ is the ionospheric projection of the magnetic drift (gradient B drift plus curvature drift) velocity of the proton fluid with the average energy W; s is the field-aligned distance, s_{e} and s_{I} are at the equator and the ionospheric height; $B(s)$ and B_{I} are the magnetic field strengths at the distances s and s_{I}, respectively. The quantity R_b represents the volume of a flux tube with unit cross-sectional area at the ionospheric height. The velocity $\bar{\nu}_{\mathrm{m,I}}$ is derived from the gradient of R_b (VASYLIUNAS, 1970; YAMAMOTO *et al.*, 1996):

$$\bar{\nu}_{\mathrm{m,I}}=-\frac{2}{3e}\frac{1}{R_b B_{\mathrm{I}}}\boldsymbol{b}_{\mathrm{I}}\times\nabla_{\mathrm{I}}R_b, \tag{3}$$

where $\boldsymbol{b}_{\mathrm{I}}$ is the unit vector parallel to the ionospheric magnetic field $\boldsymbol{B}_{\mathrm{I}}$.

In Fig. 7, the equicontours of R_b are plotted on the ionospheric plane for the '89

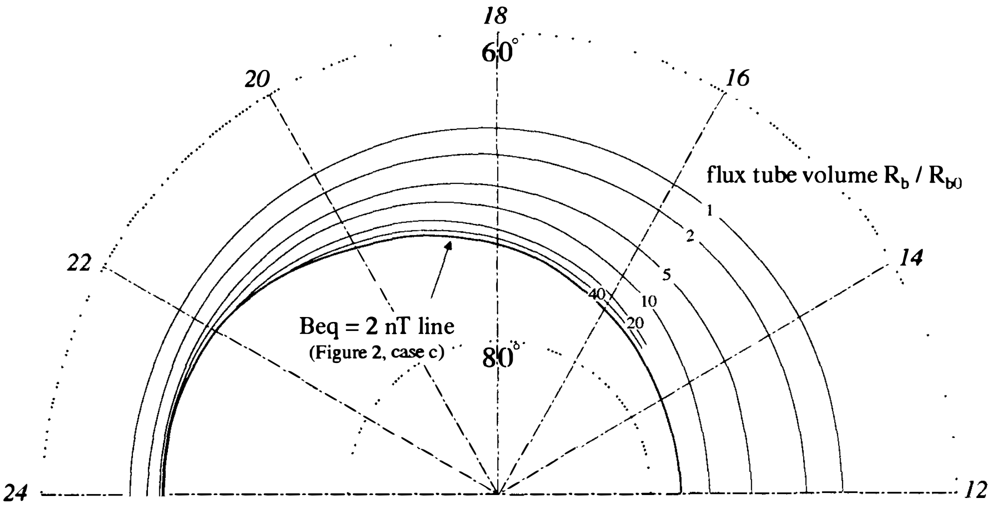

Fig. 7. Equicontours of the flux tube volume R_b, normalized by R_{b0} (for their definitions, see text), on the ionospheric plane. Superposed is the $B_{eq}=2\,nT$ line (in Fig. 2, case c).

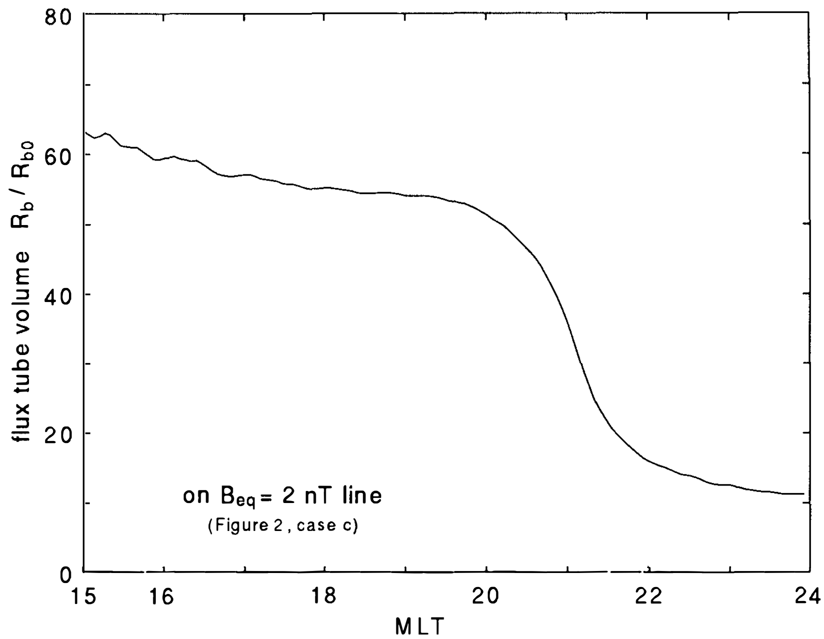

Fig. 8. Flux tube volume R_b/R_{b0} varying along the $B_{eq}=2\,nT$ line (in Fig. 2, case c).

Tsyganenko model with $K_p=0$ and $B_{Z,\,\text{ext}}=-4$ nT added. Here R_b is normalized by a value of R_b, R_{b0}, for the dipole field lines with the equatorial distance of 7 Earth radii: $R_{b0}=1.32\times10^{10}$ m. Superposed is the contour of $B_{eq}=2$ nT in case of $B_{Z,\,\text{ext}}=-4$ nT (in Fig. 2). Figure 8 shows that the flux tube volume R_b on the $B_{eq}=2$ nT line significantly increases with decreasing MLT, in the interval between 24 and about 20 MLT, with a total increase by a factor of 4.4. (This increase of R_b is essentially attributed to the increase of the field line length. Detailed discussion is given in Appendix.) From the dawn-dusk symmetry of our magnetic field model, it follows that R_b on the nightside (20–4 MLT) injection boundary is minimized around midnight and increased toward dawn or dusk. Considering the (above-mentioned) local time dependence of the ion energy density, as a simple model we assume that the flux tube energy content, $\varepsilon = (3p/2)\ R_b$, is constant on the nightside injection boundary. Under this assumption, $J_{\parallel\mathrm{i}}$ on the nightside injection boundary is determined by the component of $\bar{\nu}_{\mathrm{m,i}}$ perpendicular to the injection boundary as well as the gradient of ε perpendicular to it (see eq. (1)). Integrating $J_{\parallel\mathrm{i}}$ across the nightside injection boundary (in the perpendicular direction), the FAC intensity, I, is approximately given by

$$I \sim e\ (\bar{\nu}_{\mathrm{m,i}})_{\perp}[\varepsilon], \tag{4}$$

where $(\bar{\nu}_{\mathrm{m,i}})_{\perp}$ is the equatorward component (perpendicular to the injection boundary) of $\bar{\nu}_{\mathrm{m,i}}$, and $[\varepsilon]$ is the net change (>0) of ε across the boundary. The perpendicular components of $\bar{\nu}_{\mathrm{m,i}} \times (1\ \mathrm{keV})$ on the $B_{\mathrm{eq}} = 2$ nT line (covering the nightside injection boundary) for the case of $K_p = 0$ and $B_{Z,\,\mathrm{ext}} = -4$ nT are plotted in Fig. 9. It is found that on the nightside injection boundary, $\bar{\nu}_{\mathrm{m,i}}$ has an equatorward component on the

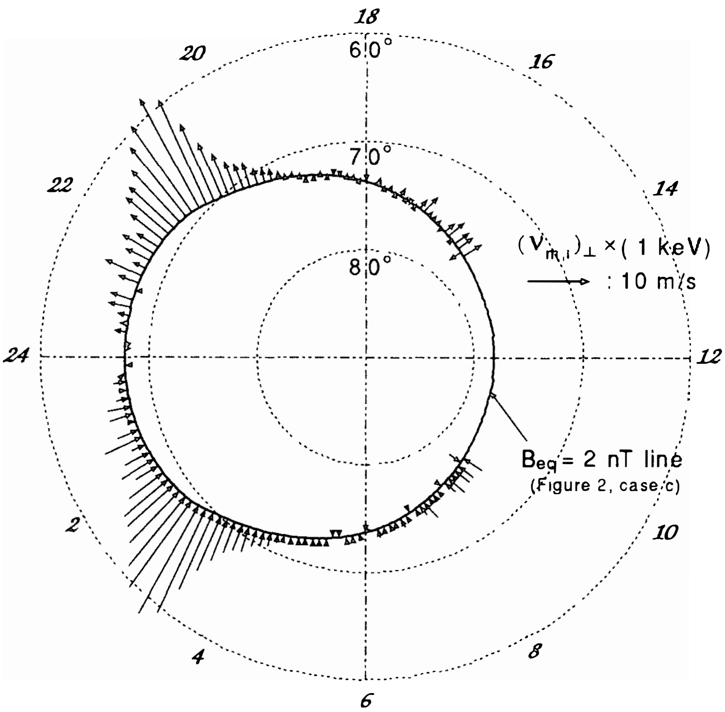

Fig. 9. Perpendicular (to the $B_{\mathrm{eq}} = 2\,nT$ line) component of the average magnetic drift velocity, $(\bar{\nu}_{\mathrm{m,i}})_{\perp} \times (1\ keV)$, projected to the ionosphere, for an ion fluid with isotropic pressure and an average energy of 1 keV is plotted along the $B_{\mathrm{eq}} = 2\,nT$ line (in Fig. 2, case c). (Over the interval of 17–15 MLT, $(\bar{\nu}_{\mathrm{m,i}})_{\perp}$ changes irregularly and sometimes its direction is reversed, i.e., directed poleward, although in reality $(\bar{\nu}_{\mathrm{m,i}})_{\perp}$ must be invariably directed equatorward in the case of this figure. The cause of such irregularities in $(\bar{\nu}_{\mathrm{m,i}})_{\perp}$ is explained as follows: Basically, within a limited computational time it is difficult to find (for any local time) such a field line as having B_{eq} extremely close to a given value of $2\,nT$. On the field lines actually identified as those on the $B_{\mathrm{eq}} = 2\,nT$, the values of B_{eq} can deviate, at most 5%, from $2\,nT$. Irregular deviation (from $2\,nT$) of B_{eq} causes such irregularities in R_b as shown in Fig. 8, leading to irregularities in $(\bar{\nu}_{\mathrm{m,i}})_{\perp}$.)

duskside and a poleward one on the dawnside. Such a property of $\bar{\nu}_{m,i}$ (*i.e.*, distortion) on the nightside injection boundary is commonly found under other conditions of the '89 Tsyganenko model with low K_p values and $B_{Z,\mathrm{ext}}$ of minus a few nanoTeslas added, which is shown in Fig. 10. (As would be expected, it is found that the outer boundary of the firmly closed region is located at lower latitudes as K_p or $-B_{Z,\mathrm{ext}}$ increases.) On investigation of the same (in $B_{Z,\mathrm{ext}}$ *and* K_p) cases as Figs. 9 and 10, we observe similar distortion (not shown), in the nightside sector, on the $B_{\mathrm{eq}}=1$ nT and 3 nT lines too, although the MLT range of distortion on the $B_{\mathrm{eq}}=1$ nT line is slightly narrower than that on the $B_{\mathrm{eq}}=2$ nT line. Consequently, the FACs of region 1 sense can be generated around the nightside injection boundary when the flux tube energy content $[\varepsilon]$ has an equatorward gradient there. As a numerical example, we assume that R_b/R_{b0}~31 and

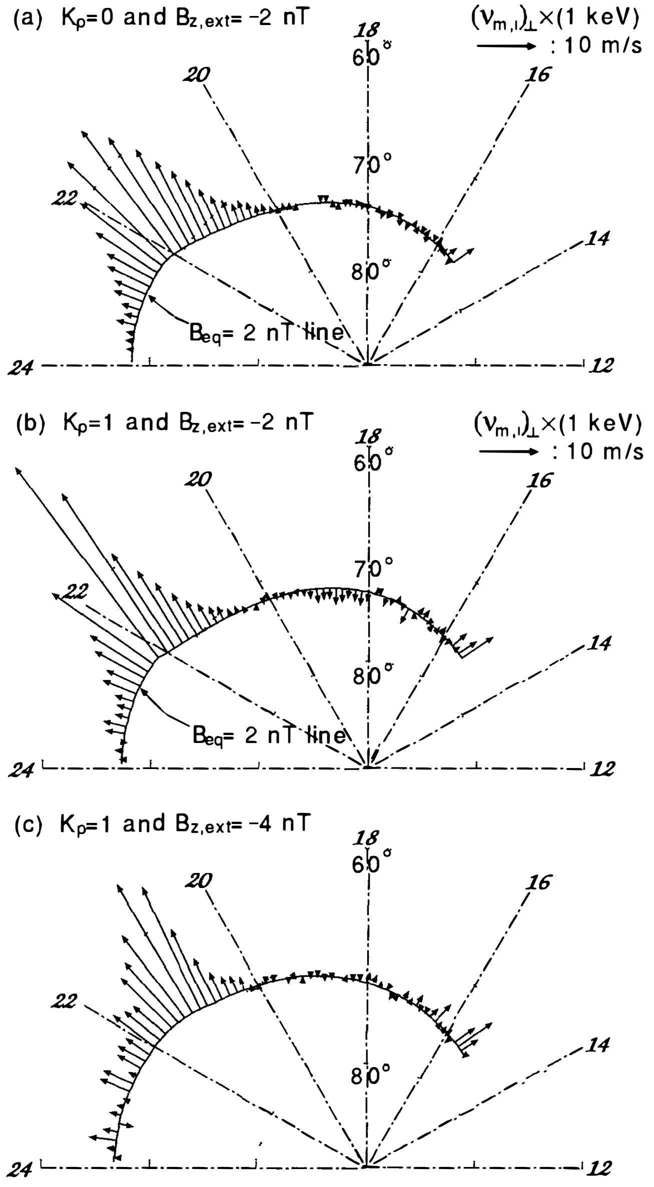

Fig. 10. Same format as in Fig. 9, but for (a) $K_p=0$ and $B_{Z,\mathrm{ext}}=-2\,nT$, (b) $K_p=1$ and $B_{Z,\mathrm{ext}}=-2\,nT$, (c) $K_p=1$ and $B_{Z,\mathrm{ext}}=-4\,nT$

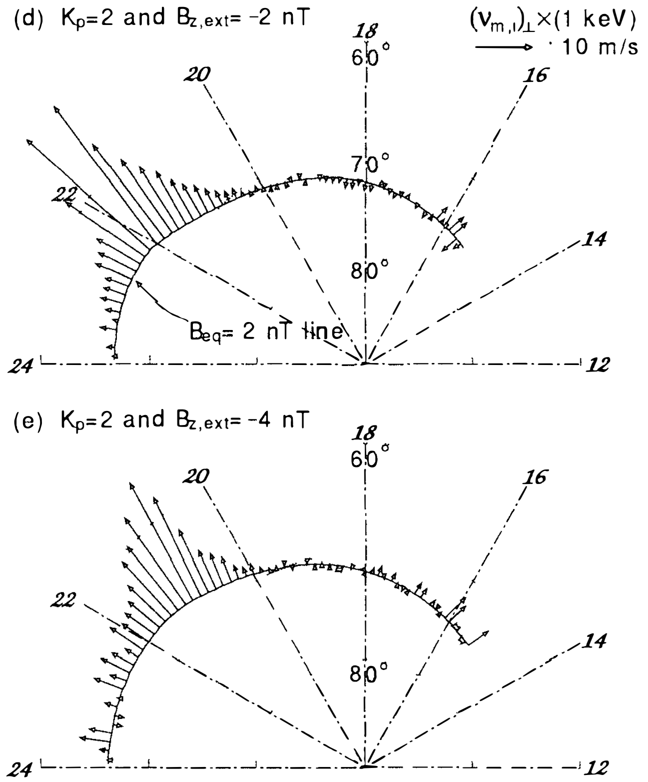

Fig. 10 (continued). (d) $K_p=2$ and $B_{Z,\mathrm{ext}}=-2$ nT, and (e) $K_p=2$ and $B_{Z,\mathrm{ext}}=-4$ nT.

$|(\bar{\nu}_{m,i})_{\perp}|$~8 m/s/keV, and that the number density and the average energy of the plasma particles just inside the injection boundary are 0.13 cm^{-3} and 3 keV, respectively. Then we may have $[\varepsilon]$~0.39 ($keV cm^{-3}$)$\times 31\ R_{b0}$, and finally the FAC intensity in eq. (4) is estimated as I~0.2 A/m. This value is comparable to a typical intensity ($\gtrsim$0.1 A/m) of the region 1 FACs observed near the poleward edge of the region of auroral particle precipitation (*e.g.*, FUKUNISHI *et al.*, 1993).

4. Conclusions

Using the Tsyganenko magnetic field model (1989), we have determined the outer boundary of the firmly closed region when the interplanetary magnetic field (IMF) is southward. As a simple model including the effect of IMF $B_Z<0$, the B_Z component of a constant value of minus a few nanoTeslas (denoted by $B_{Z,\mathrm{ext}}$) is added to the original field from the Tsyganenko model with low K_p values. As a new concept, the firmly closed region is defined as a region where any field line is invariably closed, being unperturbed by temporal IMF fluctuations with amplitudes of the order of 1 nT. In the present study, as a practical model, the outer boundary of the firmly closed region is assumed to be constituted by the field lines with an equatorial field strength, B_{eq}, of 2 nT. Interestingly, for a specific case of $K_p=0$ and $B_{Z,\mathrm{ext}}=-4$ nT, the ionospheric projection of the outer boundary of the closed region (namely the $B_{eq}=2$ nT line) coincides with a typical auroral circle, which was earlier identified from the DMSP auroral images by MENG *et al.* (1977). A most important finding is that the outer boundary of the nightside closed region is distorted in the sense that the ionospheric projection of the average magnetic drift velocity of an isotropic ion fluid has an equatorward component on the duskside boundary and a poleward one on the dawnside, respectively. It is then suggested that this boundary distortion could be responsible for the generation of the region 1 field-aligned currents with a recently revealed aspect: they are often concentrated on a narrow (in latitude) zone near the poleward edge of the nightside auroral oval.

Acknowledgments

The work of T. YAMAMOTO was supported in part by the joint research programs of Radio Atmospheric Science Center, Kyoto University, Uji, Kyoto, the Institute of Space and Astronautical Science, Sagamihara, Kanagawa, and the National Institute of Polar Research, Itabashi, Tokyo.

References

AKASOFU, S.-I., MENG, C.-I. and MAKITA, K. (1992): Changes of the size of the open field line region during substorms. Planet. Space Sci., **40**, 1513–1524.

BAUMJOHANN, W., PASCHMANN, G. and LÜHR, H. (1990): Characteristics of high-speed ion flows in the plasma sheet. J. Geophys. Res., **95**, 3801–3809.

BIRN, J., HONES, E.W., Jr., CRAVEN, J.D., FRANK, L.A., ELPHINSTONE, R.D. and STERN, D.P. (1991): On open and closed field line regions in Tsyganenko's field model and their possible associations with horse collar auroras. J. Geophys. Res., **96**, 3811–3817.

ELPHINSTONE, R.D., HEARN, D., MURPHREE, J.S. and COGGER, L.L. (1991): Mapping using the Tsyganenko magnetic field model and its relationship to Viking auroral images. J. Geophys. Res., **96**, 1467–1480.

FUKUNISHI, H., TAKAHASHI, Y., NAGATSUMA, T., MUKAI, T. and MACHIDA, S. (1993): Latitudinal structures of nightside field-aligned currents in their relationships to the plasma sheet regions. J. Geophys. Res., **98**, 11235–11255.

HRUŠKA, A. (1986): Field aligned currents in the earth plasma sheet. J. Geophys. Res., **91**, 371–374.

MENG, C.-I., HOLZWORTH, R.H. and AKASOFU, S.-I. (1977): Auroral circle-delineating the poleward boundary of the quiet auroral belt. J. Geophys. Res., **82**, 164–172.

NISHITANI, N. (1992): Magnetic field line connection between the ionosphere and the magnetosphere—auroral activity and relevant magnetic field variation at geosynchronous orbit. Ph. D Thesis for Nagoya Univ.

SAITO, Y., MUKAI, T., HIRAHARA, M., MACHIDA, S. and KAYA, N. (1992): Distribution function of precipitating ion beams with velocity dispersion observed near the poleward edge of the nightside auroral oval. Geophys. Res. Lett., **19**, 2155–2158.

TSURUTANI, B.T., SLAVIN, J.A., SMITH, E.J., OKIDA, R. and JONES, D.E. (1984): Magnetic structure of the distant geotail from -60 to -220 R_E: ISEE-3. Geophys. Res. Lett., **11**, 1–4.

TSYGANENKO, N.A. (1987): Global quantitative models of the geomagnetic field in the cislunar magnetosphere for different disturbance levels. Planet. Space Sci., **35**, 1347–1358.

TSYGANENKO, N.A. (1989): A magnetospheric magnetic field model with a warped tail current sheet. Planet. Space Sci., **37**, 5–20.

TSYGANENKO, N.A. (1995): Modeling the Earth's magnetospheric magnetic field confined within a realistic magnetopause. J. Geophys. Res., **100**, 5599–5612.

VASYLIUNAS, V.M. (1970): Mathematical models of magnetospheric convection and its coupling to the ionosphere. Particles and Fields in the Magnetosphere, ed. by B.M. MCCORMAC. Norwell, D. Reidel, 60–71.

YAMAMOTO, T. and INOUE, S. (1998): Quasi-steady production of region 1 and region 2 field-aligned currents. Proc. NIPR Symp. Upper Atmos. Phys., **11**, 106–120.

YAMAMOTO, T., KANEDA, E., HAYAKAWA, H., MUKAI, T., MATSUOKA, A., MACHIDA, S., FUKUNISHI, H., KAYA, N., TSURUDA, K. and NISHIDA, A. (1993): Meridional structures of electric potentials relevant to premidnight discrete auroras: a case study from Akebono measurements. J. Geophys. Res., **98**, 11135–11151.

YAMAMOTO, T., INOUE, S., NISHITANI, N., OZAKI, M. and MENG, C.-I. (1996): A theory for generation of the paired region 1 and region 2 field-aligned currents. J. Geopphys. Res., **101**, 27199–27222.

ZWICKL, R.D., BAKER, D.N., BAME, S.J., FELDMAN, W.C., GOSLING, J.T., HONES, E.W., Jr., MCCOMAS, D J., TSURUTANI, B.T. and SLAVIN, J.A. (1984): Evolution of the earth's distant magnetotail: ISEE 3 electron plasma results. J. Geophys. Res., **89**, 11007–11012.

(Received December 1, 1998; Revised manuscript accepted February 17, 1999)

Appendix

Here we discuss how the flux tube volume R_b (defined in eq. (2)) changes along the outer boundary of the firmly closed region, i.e, the contour of $B_{eq}=2$ nT (see Figs. 1 and 2). Figure A1 shows the projections, to (a) the X-Y, (b) the Y-Z and (c) the Z-X planes, of the field lines with ionospheric foot points at various (duskside) local times on the $B_{eq}=2$ nT line, in the case that $B_{Z,\,ext}=-4$ nT is added to the '89 Tsyganenko model with $K_p=0$. In Fig. A1a, we find that the total length of the X-Y plane projection of the field line greatly increases with decreasing MLT, between 24 and 20 MLT. In (b) and (c), the total lengths of the projections are found to increase with decreasing MLT, in the 'whole' range between 24 and 14 MLT. Therefore the total length of a field line on the $B_{eq}=2$ nT line can be expected to increase with decreasing MLT, in the whole MLT range, which is actually confirmed by calculation of the field line length (Fig. A2). The flux tube volume R_b defined for a field line depends on the length of the field line as well as the cross-sectional area of the flux tube ($\propto 1/B$), particularly in a region where the magnetic field is weak. Figure A3 shows the magnetic field strengths varying along the field lines depicted in Fig. A1. From this figure, we find that the longer field line has a

(a)

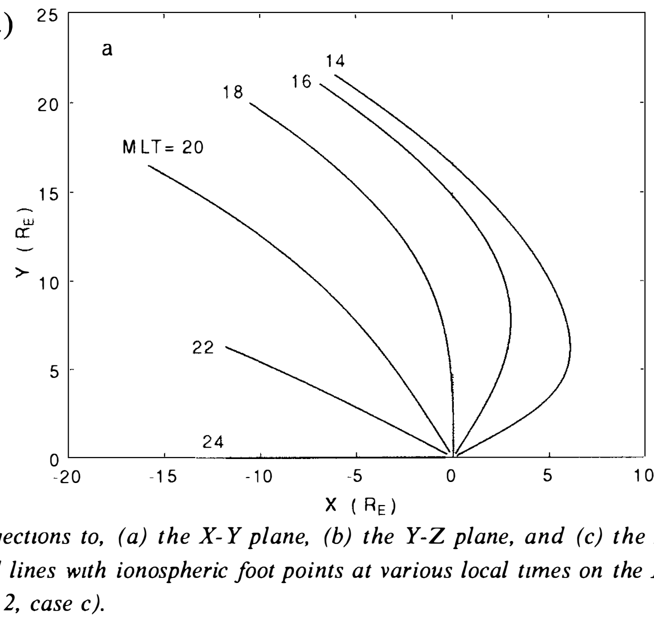

Fig. A1. Projections to, (a) the X-Y plane, (b) the Y-Z plane, and (c) the X-Z plane, of the field lines with ionospheric foot points at various local times on the $B_{eq}=2$ nT line (in Fig. 2, case c).

longer interval over which the cross-sectional area of the flux tube is large. So, essentially due to the increase of the field line length, R_b on the $B_{eq}=2$ nT line is expected to increase with decreasing MLT, in the whole MLT range, with a relatively sharp increase between 22 and 20 MLT. This is also confirmed by directly calculating R_b on the $B_{eq}=$ 2 nT line (see Fig. 8).

(b)

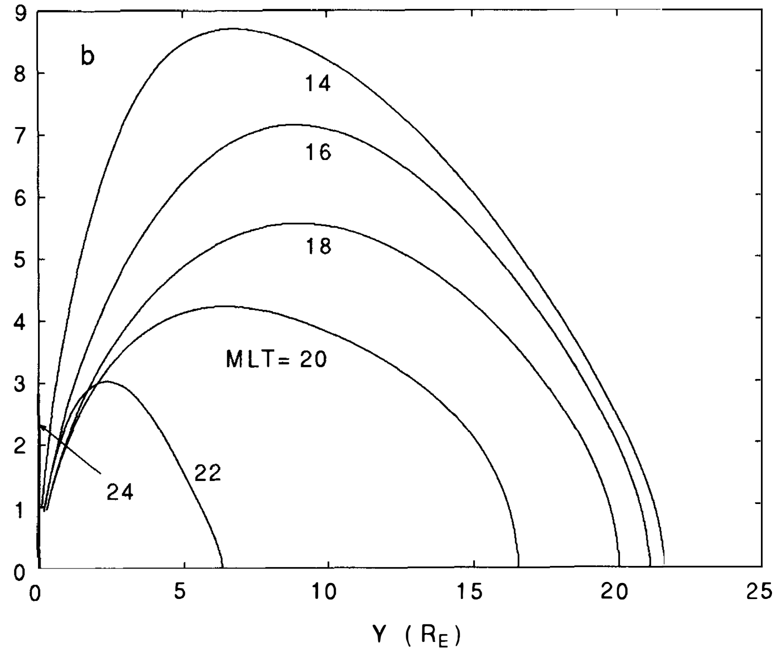

(c)

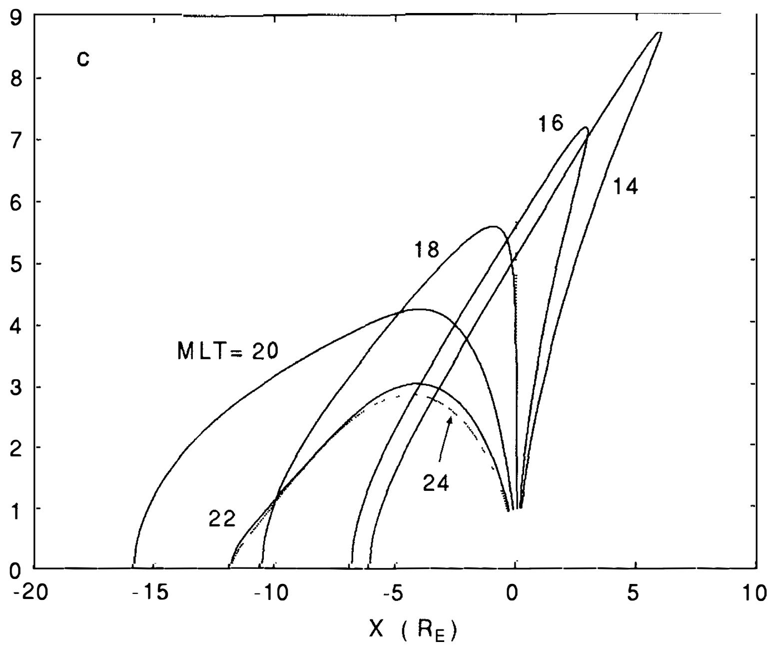

Fig. A 1 (continued).

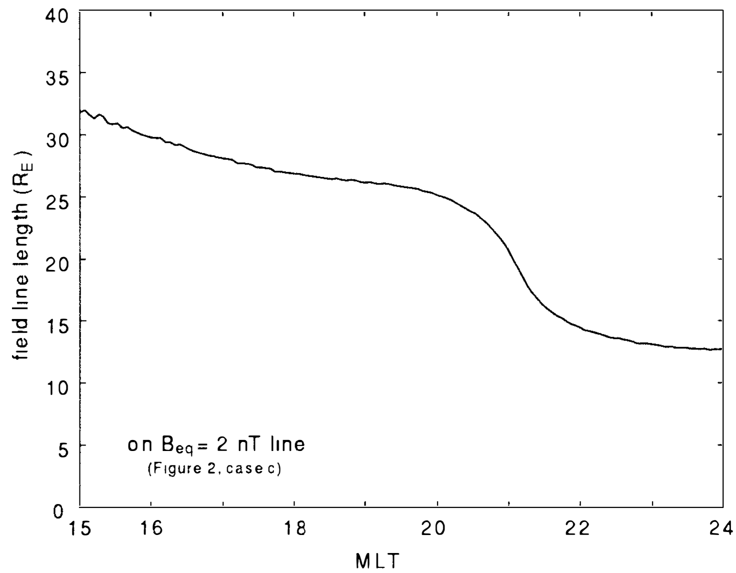

Fig. A 2. *Total length of the field line (between the ionosphere and the equator) on the $B_{eq}=2\,nT$ line (in Fig. 2, case c) plotted against (duskside) MLT.*

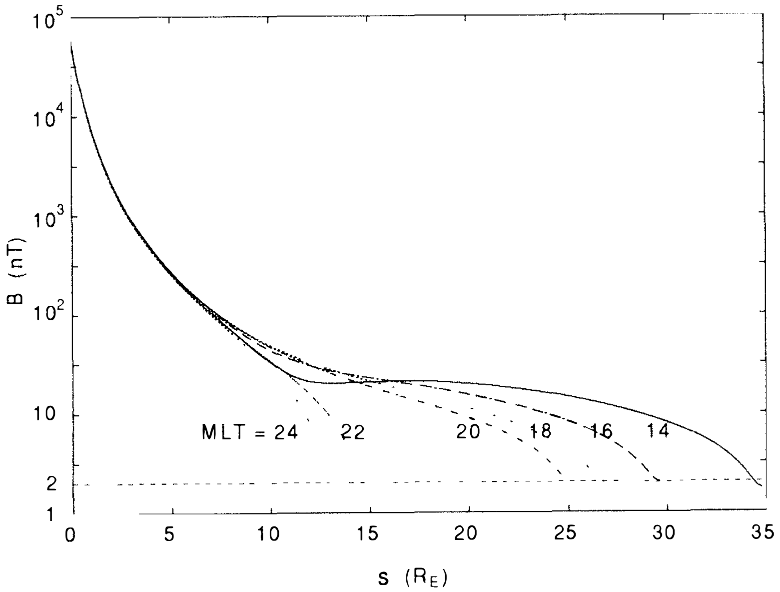

Fig. A 3. *Magnetic field strengths varying along the field lines depicted in Fig. A 1, where s is the field-aligned distance from the Earth surface.*